Available online at http://scik.org
Commun. Math. Biol. Neurosci. 2022, 2022:32
https://doi.org/10.28919/cmbn/7260
ISSN: 2052-2541

STABILITY AND BIFURCATION OF A PREY-PREDATOR SYSTEM INCORPORATING FEAR AND REFUGE

HIBA ABDULLAH IBRAHIM, DAHLIA KHALED BAHLOOL, HUDA ABDUL SATAR,

RAID KAMEL NAJI*

Department of Mathematics, College of Science, University of Baghdad, Baghdad 10071, Iraq

Abstract: It is proposed and studied a prey-predator system with a Holling type II functional response that merges predation fear with a predator-dependent prey's refuge. Understanding the impact of fear and refuge on the system's dynamic behavior is one of the objectives. All conceivable steady-states are investigated for their stability. The persistence condition of the system has been established. Local bifurcation analysis is performed in the Sotomayor sense. Extensive numerical simulation with varied parameters was used to explore the system's global dynamics. A limit cycle and a point attractor are the two types of attractors in the system. It's also interesting to note that the system exhibits bi-stability between these 2 types of attractors. Fear also has a destabilizing effect on the dynamics of the system.

Keywords: prey-predator; fear; refuge; bi-stability; bifurcation.

2010 AMS Subject Classification: 92B25, 34D20, 37G10.

---

*Corresponding author
E-mail address: rknaji@gmail.com
Received February 11, 2022

1. INTRODUCTION

Because of its global importance and existence, the dynamical behavior of prey-predator systems is a popular topic in both ecology and mathematics. A functional response, which is defined as the amount of prey consumed per predator and per unit of time, is used to characterize prey-predator dynamics. It promotes the movement of food from the lower to the upper levels [1]. The prey-predator model is diverse in that it focuses on interactions between two species with various sorts of functional responses [2-4].

All of the above-mentioned studies suggest prey-predator models that only include direct prey killing in the presence of predators and ignore the impact of predators on prey. According to certain experimental investigations, the presence of a predator can impact prey behavior even more profoundly than direct predation [5-7]. As a result, prey responded to the threat of predation by exhibiting a variety of anti-predator behaviors such as habitat alterations, foraging, attentiveness, and physiological changes.

Fear of predators produces anti-predator defenses that inhibit prey population reproduction, as demonstrated in [8]. They presented a prey-predator model that incorporates the fear element into prey reproduction and discovered that fear stabilizes the system by removing periodic solutions; nevertheless, low levels of fear can cause the Hopf bifurcation. Many researchers have presented models in this area in the subsequent years; see for example [9-10] and the references therein.

On the other hand, because prey hide in refuges to avoid predators, not all prey are caught by predators. The prey refuge must be included in the system in order to imitate the current circumstance. As a result, one of the key areas in biomathematics has been the study of a prey-predator system with prey refuge, and many scholars have made important discoveries in this area; see for example [11-13] and the references therein.

In light of the foregoing, several scholars have looked into the prey-predator system to see if it includes fear, shelter, or both. Panday et al., [14] has suggested a three-species food chain model that incorporates the cost of fear into a middle predator's predation rate. Fear, they discovered, has the ability to bring the model from chaos to a firm focus. Pal et al., [15] proposed the Leslie-Gower prey-predator model, in which predators work together to catch prey. They hypothesized that prey population exhibits anti-predator behavior in response to the threat of predation. It's also been discovered that by ignoring the existence of periodic solutions, the fear factor can help to stabilize the prey-predator system. In a prey-predator system with a gestation time delay, Kumar and Dubey, [16] established a mathematical model to examine fear's influence on prey refuge. The fear effect on the prey is thought to cause Hopf-bifurcation in the system. With a Holling-type-II prey-predator model integrating a prey refuge, Zhang et al., [17] studied the impact of anti-predator behavior due to predator fear. They discovered that at positive equilibrium, the fear effect reduces predator population density and stabilizes the system by excluding the occurrence of periodic solutions. Fear was studied in a Holling type II prey-predator model with prey refuge and supplementary food for the predator by Samaddar et al., [18]. They discovered that fear had the impact of not just reducing predator density but also driving the system toward stability. Fakhry and Naji, [19] proposed and investigated an ecological model based on a square-root prey-predator system with predator fear. They demonstrated that increasing the fear impact reduces predator density while having no effect on prey density and that the model remains in a positive equilibrium. Fear was examined by Ibrahim and Naji, [20] in a three-species Beddington–DeAngelis feeding chain model. It has been discovered that the presence of fear, up to a critical level, has a system-stabilizing impact. Otherwise, it acts as a system-wide extinction factor.

As a result, in this study, a Holling type II prey-predator system was developed and examined, which includes a fear impact due to the predator's presence and the prey's refuge, and is proportional to the number of direct interactions between the prey and predator populations. In contrast to all of the previous studies, the exponential fear function is believed to be utilized to represent the effect of fear on prey growth rate. The rest of the paper, on the other hand, is organized as follows: The mathematical formulation of the prey-predator system is discussed in the following section. Section three discusses the presence of possible steady-state points as well as their stability analyses. The local bifurcation analysis was covered in section four. The numerical simulation is found in section five. Section six concludes with a discussion and conclusion.

2. MATHEMATICAL MODEL

In this part, a mathematical model of the Holling type II prey-predator is developed, with predator-dependent refugia and prey fear as factors. In the absence of the predator, the prey is thought to expand logistically, while the predator decays exponentially in the absence of their prey. Furthermore, the number of refugia is proportional to the number of direct interactions between the prey population $X(T)$ and the predator population $Y(T)$, where C denotes the intensity of the interaction, allowing the rest of the prey population $X(1-CY)$ to be predated, where $C \in [0,1]$. As a result, only those values of C that $Y \leq \frac{1}{C}$ are allowed from now on, ensuring the authorized range of refuge $0 \leq 1 - CY \leq 1$ for a realistic environment [21]. In addition, the prey's fear of predation is taken into account by using the $\exp(-K_1 Y)$ function, which measures the probability of the prey's growth in the presence of the predator, with K_1 standing for the fear factor. As a result, the dynamics of the aforementioned prey-predator model can be represented by the differential equations shown below.

$$
\begin{aligned}
\frac{dX}{dT} &= Re^{-K_1 Y} X\left(1 - \frac{X}{K_0}\right) - \frac{AX(1-CY)Y}{B + X(1-CY)}, \\
\frac{dY}{dT} &= \frac{EAX(1-CY)Y}{B + X(1-CY)} - DY,
\end{aligned} \tag{1}
$$

where $X(0) \geq 0$ and $Y(0) \geq 0$. The parameters, however, can be found in the Table (1) below.

Table 1: Parameters description

Parameter	Description
R	The internist growth rate of prey
K_0	The carrying capacity of the environment
K_1	The prey’s fear rate
A	The maximum attack rate
B	The half saturation constant
C	The intensity of the prey-predator interaction
E	The conversion rate
D	The predator natural death rate

Obviously, the function $e^{-K_1 Y}$ describes the influence of prey's fear of the predation process, which reduces prey reproduction, hence it meets the following properties:

1. When $K_1 = 0$ or $Y = 0$, then $e^{-K_1 Y} = 1$. As a result, the prey's growth will be unaffected.
2. $\lim_{K_1 \to \infty} e^{-K_1 Y} = \lim_{Y \to \infty} e^{-K_1 Y} = 0$, accordingly, the prey's growth is completely halted.
3. $\frac{\partial e^{-K_1 Y}}{\partial K_1} < 0$, hence the growth of the prey decrease due to the increasing in the anti-predator behavior. Similarly, as $\frac{\partial e^{-K_1 Y}}{\partial Y} < 0$, the growth of the prey decrease due to the increasing in the population of the predator.

Now in order to study the above system of equations, the following dimensionless variables and parameters are used.

$$t = RT,\ x = \frac{X}{K_0},\ y = CY,\ w_0 = \frac{K_1}{C},\ w_1 = \frac{A}{CRK_0},\quad w_2 = \frac{EA}{R}\ ,\ w_3 = \frac{D}{R},\ w_4 = \frac{B}{R}.$$

Therefore, the following dimensionless system is obtained.

$$\begin{aligned} \frac{dx}{dt} &= e^{-w_0 y} x(1-x) - \frac{w_1 x(1-y)y}{w_4 + x(1-y)}, \\ \frac{dy}{dt} &= \frac{w_2 x(1-y)y}{w_4 + x(1-y)} - w_3 y. \end{aligned} \tag{2}$$

Therefore, $R_+^2 = \{(x,y) \in R^2 | x \geq 0, y \geq 0\}$ is obviously the domain of system (2). Furthermore, the system (2) contains C^1 functions, indicating that these are Lipschitzain functions. As a result, the system (2) solution exists and is unique. In addition, the following theorem establishes that the solutions of the system (2) are uniformly bounded.

Theorem 1: The system (2) has solutions that are uniformly bounded.

Proof. Let $(x(t), y(t))$ be any solution of system (2), then from the first equation it is observed that

$$\frac{dx}{dt} \leq e^{-w_0 y} x(1-x) \leq x(1-x)$$

Then, direct computation gives that $x \leq 1$. Let now that $M(t) = x(t) + y(t)$ then

$$\frac{dM}{dt} \leq e^{-w_0 y} x(1-x) - w_3 y \leq 2x - \rho(x+y) \leq 2 - \rho M,$$

where $\rho = \min\{1, w_3\}$. Therefore, as $t \to \infty$ it is got that $x + y \leq \frac{2}{\rho}$. Hence the proof is complete.

3. Existence of Steady-State Points and Their Stability

This section discusses the existence of steady-state points in the system (2), as well as their local stability analysis, so that the following requirements can be constructed for each of these steady-state points:

The trivial steady-state point (TSSP) that is given by $E_0 = (0,0)$ is always present.

In the absence of predation, the axial steady-state point (ASSP) is always present and is given by $E_1 = (1, 0)$ when the prey population grows to the carrying capacity.

The solutions of the following algebraic system are represented by the coexistence or positive steady-state points (PSSP) of the system (2):

$$\begin{aligned} g_1(x,y) &= e^{-w_0 y}(1-x) - \frac{w_1(1-y)y}{w_4 + x(1-y)} = 0, \\ g_2(x,y) &= \frac{w_2 x(1-y)}{w_4 + x(1-y)} - w_3 = 0. \end{aligned} \tag{3}$$

Straightforward computation gives that

$$x = \frac{w_3 w_4}{(w_2 - w_3)(1-y)}. \tag{4}$$

Substituting the acquired value of x, which is positive when $w_2 > w_3$, in the first equation of (3) yields the transcendental equation shown below.

$$\begin{aligned} f(y) = {} & w_1(w_2 - w_3)^2 y^3 - 2w_1(w_2 - w_3)^2 y^2 \\ & +[w_1(w_2 - w_3) + w_2 w_4 e^{-w_0 y}](w_2 - w_3)y \\ & -[(w_2 - w_3) - w_3 w_4]w_2 w_4 e^{-w_0 y} = 0. \end{aligned} \tag{5}$$

Equation (5) clearly becomes an algebraic polynomial equation of degree three for $w_0 = 0$. The discard rule of sign indicates that the obtained algebraic polynomial of the third degree has either three or one positive root if:

$$w_3 w_4 < (w_2 - w_3) \tag{6}$$

In the situation of $w_0 > 0$, however, the equation (5) is a transcendental equation with one, no, or an infinite number of roots, depending on the form of $f(y)$.

Since $f(0) = -[(w_2 - w_3) - w_3 w_4] w_2 w_4$ is negative under condition (6), and $f(1) = w_2 w_3 {w_4}^2 e^{-w_0} > 0$. Then as a result of the intermediate value theorem, at least one positive root between 0 and 1 will exist.

As a result, if condition (6) applies, the system (2) has at least one PSSP given by $E_2 = (x^*, y^*)$, where x^* is defined by equation (4) and y^* is the root of equation (5).

The Jacobian matrix of the system (2) about any point (x, y) now looks like this:

$$J = \left[\rho_{ij}\right]_{2\times 2}, \tag{7}$$

where

$$\rho_{11} = g_1 + x\left[-e^{-w_0 y} + \frac{w_1(1-y)^2 y}{[w_4 + x(1-y)]^2}\right],$$

$$\rho_{12} = x\left[-w_0 e^{-w_0 y}(1-x) - \frac{w_1 w_4(1-2y) + w_1 x(1-y)^2}{[w_4 + x(1-y)]^2}\right],$$

$$\rho_{21} = y\left[\frac{w_2 w_4(1-y)}{[w_4 + x(1-y)]^2}\right],$$

$$\rho_{22} = g_2 + y\left[-\frac{w_2 w_4 x}{[w_4 + x(1-y)]^2}\right],$$

with g_1 and g_2 are given in equation (3).

Accordingly, the Jacobian matrix of the system (2) at TSSP is determined by

$$J(E_0) = \begin{bmatrix} 1 & 0 \\ 0 & -w_3 \end{bmatrix}. \tag{8}$$

Therefore, the eigenvalues of $J(E_0)$ are $\lambda_{01} = 1$ and $\lambda_{02} = -w_3$, and hence TSSP is a saddle point.

The Jacobian matrix of the system (2) at ASSP is given by:

$$J(E_1) = \begin{bmatrix} -1 & -\frac{w_1}{(w_4+1)} \\ 0 & \frac{w_2}{(w_4+1)} - w_3 \end{bmatrix}. \tag{9}$$

Clearly the eigenvalues of $J(E_1)$ are determined by

$$\lambda_{11} = -1 \text{ and } \lambda_{12} = \frac{w_2}{(w_4+1)} - w_3. \tag{10}$$

Hence all the eigenvalues of $J(E_1)$ have negative real parts and the ASSP is locally asymptotically stable provided that:

$$w_2 < w_3(w_4 + 1). \tag{11}$$

Now the Jacobian matrix of the system (2) at the PSSP can be written as:

$$J(E_2) = [b_{ij}]_{2\times 2}, \tag{12}$$

where

$$b_{11} = x^* \left[-e^{-w_0 y^*} + \frac{w_1(1-y^*)^2 y^*}{[w_4+x^*(1-y^*)]^2} \right],$$

$$b_{12} = x^* \left[-w_0 e^{-w_0 y^*}(1-x^*) - \frac{w_1 w_4 (1-2y^*) + w_1 x^* (1-y^*)^2}{[w_4+x^*(1-y^*)]^2} \right],$$

$$b_{21} = y^* \left[\frac{w_2 w_4 (1-y^*)}{[w_4+x^*(1-y^*)]^2} \right],$$

$$b_{22} = -y^* \left[\frac{w_2 w_4 x^*}{[w_4+x^*(1-y^*)]^2} \right].$$

Direct computation gives that the eigenvalues of $J(E_2)$ are given by the roots of the following second degree polynomial equation:

$$\lambda^2 - T\lambda + D = 0, \tag{13}$$

where $T = b_{11} + b_{22}$, and $D = b_{11}b_{22} - b_{12}b_{21}$. Therefore, the roots of the equation (13) are given by:

$$\lambda_{21} = \frac{T}{2} + \frac{1}{2}\sqrt{T^2 - 4D};\ \lambda_{22} = \frac{T_3}{2} - \frac{1}{2}\sqrt{T^2 - 4D}. \tag{14}$$

Accordingly the following theorem can be proved easily.

Theorem 2. The PSSP of system (2) is locally asymptotically stable if and only if.

$$\frac{w_1(1-y^*)^2 y^*}{[w_4+x^*(1-y^*)]^2} < e^{-w_0 y^*}, \tag{15a}$$

$$\frac{w_4 + x^*(1-y^*)^2}{w_4 y^*} > 2. \tag{15b}$$

Proof. According to the forms of the eigenvalues λ_{21} and λ_{22}, which are given in equation (14), they have negative real parts and hence PSSP is locally asymptotically stable if and only if the sufficient conditions (15a) and (15b) are satisfied.

The persistence of the system (2) is investigated in the following part. It is well knowledge that the system will continue to exist if and only if none of their species become extinct. This means that the system (2) survives if the system's trajectory, which starts at a positive point, does not have an omega limit set on the domain's border axis.

The Dulac function is now employed to determine the possibility of periodic dynamics in the interior of the positive quadrant of the $xy-$ plane.

Consider the following function $H(x,y)=\frac{1}{xy}$. Note that the function $H(x,y)>0$ and it is C^1 function in the interior of $\mathbb{R}_+^{\;2}$ of $xy-$plane. Moreover, it is obvious that:

$$\Delta(x,y)=\frac{\partial}{\partial x}(H\cdot xg_1)+\frac{\partial}{\partial y}(H\cdot yg_2)=-\frac{e^{-w_0y}}{y}+\frac{w_1(1-y)^2-w_2w_4}{[w_4+x(1-y)]^2}. \tag{16}$$

Therefore, $\Delta(x,y)$ does not vary sign and does not vanish under the following sufficient condition:

$$w_1(1-y)^2\le w_2w_4. \tag{17}$$

Theorem 3: If no periodic dynamics exist in the interior of the positive quadrant, the system (2) is uniformly persistent if the following condition is met.

$$w_3(w_4+1)<w_2. \tag{18}$$

Proof. Define a function $\vartheta(x,y)=x^{p_1}y^{p_2}$, where p_1,p_2 are positive constants, and $\vartheta(x,y)>0$ for all $(x,y)\in Int\,\mathbb{R}_+^{\;2}$ of $xy-$plane with $\vartheta(x,y)=0$ if any one of x or y approaches zero. Therefore, straightforward computation yields:

$$\Omega(x,y)=\frac{\vartheta'(x,y)}{\vartheta(x,y)}=p_1g_1+p_2g_2,$$

where the functions $g_i; i=1,2$, are given in the equation (3). Note that, because there are no periodic dynamics in the interior of the positive quadrant, the proof is satisfied if $\Omega(x,y)>0$ for all border steady-state points, according to the average Lyapunov method.

Therefore, by using equation (3) we obtain that

$$\Omega(E_0)=p_1[1]+p_2[-w_3].$$

Obviously, by selecting the arbitrary positive constant of p_1 sufficiently larger than that of p_2, it is obtained that $\Omega(E_0)>0$.

$$\Omega(E_1)=p_2[\frac{w_2}{w_4+1}-w_3].$$

Note that, the condition (18) guarantees that $\Omega(E_1)>0$. Hence the proof is done.

The global stability is studied for all locally stable steady-state points as shown in the following theorems.

Theorem 4. If the ASSP of system (2) is locally asymptotically stable in R^2_+, then it is globally asymptotically stable if and only if

$$\frac{w_2}{w_4} < w_3. \tag{19}$$

Proof. Let $V = c_1\,(x - 1 - \ln x) + c_2 y$ be a real valued function, where c_1 and c_2 are positive constants. Direct computation shows that $V(1,0) = 0$ and $V(x,y) > 0$ for all $(x,y) \in R^2_+$ and $(x.y) \neq (1,0)$ with $x > 0$ and $y \geq 0$. Therefore the function V is a positive definite function.

Furthermore, the derivative of V can be written as

$$\frac{dV}{dt} = -c_1 e^{-w_0 y}(x-1)^2 - \frac{(c_1 w_1 - c_2 w_2)(1-y)xy}{w_4 + x(1-y)} + \frac{c_1 w_1 (1-y) y}{w_4 + x(1-y)} - c_2 w_3 y.$$

Then by choosing $c_1 = w_2$ and $c_2 = w_1$ we obtain that

$$\frac{dV}{dt} \leq -w_1 e^{-w_0 y}(x-1)^2 - \left[w_1\left(w_3 - \frac{w_2}{w_4}\right)\right] y.$$

Clearly under the condition (19), the derivative $\frac{dV}{dt}$ is negative definite.

Moreover, since V is radially unbounded function, then the ASSP is a global asymptotically stable. Recall that, because system (2) could have multiple PSSPs with unknown forms, the global stability of this steady-state point can't be studied theoretically, thus we'll analyze it numerically.

4. LOCAL BIFURCATION

In the following, Sotomayor's theorem [22] is used to study the local bifurcation that may occur around the non-hyperbolic steady-state point. The goal is to understand how changing parameter values affect the system's dynamical behavior when the parameter goes through the value that transitions the steady-state from hyperbolic to non-hyperbolic.

Now, rewrite system (2) as follows

$$\frac{d\boldsymbol{X}}{dt} = F(\boldsymbol{X}), \text{ with } \boldsymbol{X} = (x,y)^T \text{ and } \boldsymbol{F} = (xg_1, yg_2)^T.$$

Then the second directional derivative of $\boldsymbol{F}$ with respect to $\boldsymbol{X}$ can be determined as

$$D^2F.(U,U) = [c_{i1}]_{2\times 1}, \tag{20}$$

where

$$c_{11} = -2\left[e^{-w_0 y} - \frac{w_1 w_4 (1-y)^2 y}{[w_4 + x(1-y)]^3}\right] {u_1}^2$$
$$-2\left[w_0(1-2x)e^{-w_0 y} + \frac{w_1 w_4 [w_4(1-2y) + x(1-y)]}{[w_4 + x(1-y)]^3}\right] u_1 u_2$$
$$+\left[{w_0}^2 x(1-x) e^{-w_0 y} + 2\frac{w_1 w_4 x (w_4 + x)}{[w_4 + x(1-y)]^3}\right] {u_2}^2,$$

$$c_{21} = -2\left[\frac{w_2 w_4 (1-y)^2 y}{[w_4 + x(1-y)]^3}\right] {u_1}^2 + 2\left[\frac{w_2 w_4 [w_4(1-2y) + x(1-y)]}{[w_4 + x(1-y)]^3}\right] u_1 u_2$$
$$-2\left[\frac{w_2 w_4 x (w_4 + x)}{[w_4 + x(1-y)]^3}\right] {u_2}^2,$$

here $U = (u_1, u_2)^T$ be a general vector.

Theorem 6. Assume that $w_3 = \frac{w_2}{w_4 + 1} (\equiv {w_3}^*)$, then system (2) at ASSP has a transcritical bifurcation.

Proof. Note that, when $w_3 = {w_3}^*$, then the Jacobian matrix of the system (2) at ASSP can be written as

$$J_1 = J(E_1, {w_3}^*) = \begin{bmatrix} -1 & -\frac{w_1}{w_4 + 1} \\ 0 & 0 \end{bmatrix}$$

Clearly the eigenvalues of J_1 are $\lambda_{11}^* = -1$ and $\lambda_{12}^* = 0$, hence E_1 is non-hyperbolic point.

Let $\boldsymbol{U_1} = (u_{11}, u_{12})^T$ be the eigenvector of J_1 corresponding to $\lambda_{12}^* = 0$ .Then simple computation gives that $\boldsymbol{U_1} = \left(-\frac{w_1}{w_4 + 1} u_{12}, u_{12}\right)^T$, where $u_{12} \neq 0$ is any real number.

Also, let $\boldsymbol{\Psi_1} = (\psi_{11}, \psi_{12})^T$ that represents the eigenvector of ${J_1}^T$ corresponding to $\lambda_{12}^* = 0$. Then again simple calculation shows that $\boldsymbol{\Psi_1} = (0, \psi_{12})^T$, where $\psi_{12} \neq 0$ is any real number.

Since $\frac{\partial \boldsymbol{F}}{\partial w_3} = (0, -y)^T$, hence we obtain that $\boldsymbol{F}_{w_3}(E_1, {w_3}^*) = (0,0)^T$. Therefore, ${\boldsymbol{\Psi_1}}^T \left[\boldsymbol{F}_{w_3}(E_1, {w_3}^*)\right] = 0$.

Thus the system (2) at E_1 with $w_3 = {w_3}^*$ satisfies the first condition of a transcritical bifurcation in view of Sotomayor theorem. Moreover, since

$${\boldsymbol{\Psi_1}}^T \left[D\boldsymbol{F}_{w_3}(E_1, {w_3}^*)\, \boldsymbol{U_1}\right] = -u_{12} \psi_{12} \neq 0,$$

Now, ${\boldsymbol{\Psi_1}}^T [D^2 \boldsymbol{F}(E_1, {w_3}^*)(\boldsymbol{U_1}, \boldsymbol{U_1})] = -2\frac{w_2 w_4}{(w_4 + 1)^2} \psi_{12} {u_{12}}^2 \left[\frac{w_1}{w_4 + 1} + 1\right] \neq 0$, hence system (2) undergoes a transcritical bifurcation near E_1 when $w_3 = {w_3}^*$.

Theorem 7. Assume that condition (15a) holds a long with the following condition

$$\frac{w_0 e^{-w_0 y^*}(1-x^*)[w_4+x^*(1-y^*)]^2}{w_1 w_4 y^*}+\frac{w_4+x^*(1-y^*)^2}{w_4 y^*}<2. \tag{21}$$

Then as $w_1 = w_1{}^*$ system (2) has a saddle-node bifurcation at PSSP provided that

$$\beta_2 c_{11}{}^* + c_{21}{}^* \neq 0, \tag{22}$$

where all the new symbols are given in the proof, while

$$w_1{}^* = \frac{e^{-w_0 y^*}[w_4+x^*(1-y^*)][w_0(1-x^*)(1-y^*)+x^*]}{(1-y^*)(2y^*-1)}. \tag{23}$$

Proof. From the Jacobian matrix of system (2) at PSSP that is given by equation (12), it is easy to verify that $D = 0$, where D represents the determinant of $J(E_2)$ given in equation (13). So, according to the characteristic equation (13) there is a zero eigenvalue and hence, E_2 is a non-hyperbolic steady-state point. Therefore, the Jacobian matrix at $(E_2, w_1{}^*)$ can be written as

$$J_2 = J(E_2, w_1{}^*) = \begin{bmatrix} b_{11}{}^* & b_{12}{}^* \\ b_{21} & b_{22} \end{bmatrix},$$

where $b_{11}{}^* = b_{11}(w_1{}^*)$, $b_{12}{}^* = b_{12}(w_1{}^*)$ with $b_{ij}; i,j = 1,2$ are the elements of $J(E_2)$.

Let $\boldsymbol{U_2} = (u_{21}, u_{22})^T$ be the eigenvector of J_2 .Then simple computation gives that $\boldsymbol{U_2} = (\beta_1 u_{22}, u_{22})^T$, where $u_{22} \neq 0$ is any real number with $\beta_1 = -\frac{b_{12}{}^*}{b_{11}{}^*} > 0$.

Also, let $\boldsymbol{\Psi_2} = (\psi_{21}, \psi_{22})^T$ represents the eigenvector of $J_2{}^T$. Then again simple calculation shows that $\boldsymbol{\Psi}_2 = (\beta_2 \psi_{22}, \psi_{22})^T$, where $\psi_{22} \neq 0$ is any real number with $\beta_2 = -\frac{b_{21}}{b_{11}{}^*} > 0$.

Since $\frac{\partial \boldsymbol{F}}{\partial w_1} = \left(-\frac{x(1-y)y}{w_4+x(1-y)}, 0\right)^T$, hence we obtain that $\boldsymbol{F}_{w_1}(E_2, w_1{}^*) = \left(-\frac{x^*(1-y^*)y^*}{w_4+x^*(1-y^*)}, 0\right)^T \neq \boldsymbol{0}$.

Consequently, the first condition of saddle-node bifurcation in view Sotomayor theorem is satisfied. Now, since

$$D^2\boldsymbol{F}(E_2, w_1{}^*).(\boldsymbol{U_2}, \boldsymbol{U_2}) = u_{22}{}^2[c_{i1}{}^*]_{2\times 1},$$

where

$$\begin{aligned} c_{11}{}^* = &-2\left[e^{-w_0 y^*} - \frac{w_1{}^* w_4 (1-y^*)^2 y^*}{[w_4+x^*(1-y^*)]^3}\right]\beta_1{}^2 \\ &-2\left[w_0(1-2x^*)e^{-w_0 y^*} + \frac{w_1{}^* w_4 [w_4(1-2y^*)+x^*(1-y^*)]}{[w_4+x^*(1-y^*)]^3}\right]\beta_1 \\ &+\left[w_0{}^2 x^*(1-x^*)e^{-w_0 y^*} + 2\frac{w_1{}^* w_4 x^*(w_4+x^*)}{[w_4+x^*(1-y^*)]^3}\right], \end{aligned}$$

$$c_{21}{}^{*} = -2\left[\frac{w_2 w_4 (1-y^*)^2 y^*}{[w_4 + x^*(1-y^*)]^3}\right]\beta_1{}^2 + 2\left[\frac{w_2 w_4 [w_4(1-2y^*) + x^*(1-y^*)]}{[w_4 + x^*(1-y^*)]^3}\right]\beta_1 -2\left[\frac{w_2 w_4 x^*(w_4 + x^*)}{[w_4 + x^*(1-y^*)]^3}\right].$$

Therefore, $\boldsymbol{\Psi}_2{}^T D^2 \boldsymbol{F}(E_2, w_1{}^*).(\boldsymbol{U_2}, \boldsymbol{U_2}) = [\beta_2 c_{11}{}^* + c_{21}{}^*] u_{22}{}^2 \psi_{22}$. Clearly, due to condition (22), $\boldsymbol{\Psi}_2{}^T [D^2 \boldsymbol{F}(E_2, w_1{}^*)(\boldsymbol{U_2}, \boldsymbol{U_2})] \neq 0$. Hence system (2) undergoes a saddle-node bifurcation near the PSSP.

5. NUMERICAL SIMULATION

In this section, the global dynamics of the system (2) are numerically studied in this part with a hypothetical set of physiologically acceptable parameters. The goals are to corroborate the theoretical findings and to comprehend the impact of changing the parameters on the system's dynamical behavior. All numerical results are given in the form of phase portraits and time series using Matlab version R2013a. However, Mathematica 12 is used to obtain the direction field of the system (2). With the following set of parameters, different initial values are employed, and phase portraits of the resultant trajectories, as well as their direction fields, are generated in Figure (1).

$$w_0 = 0.1,\ w_1 = 1,\ w_2 = 0.5,\ w_3 = 0.1,\ w_4 = 0.2. \tag{24}$$

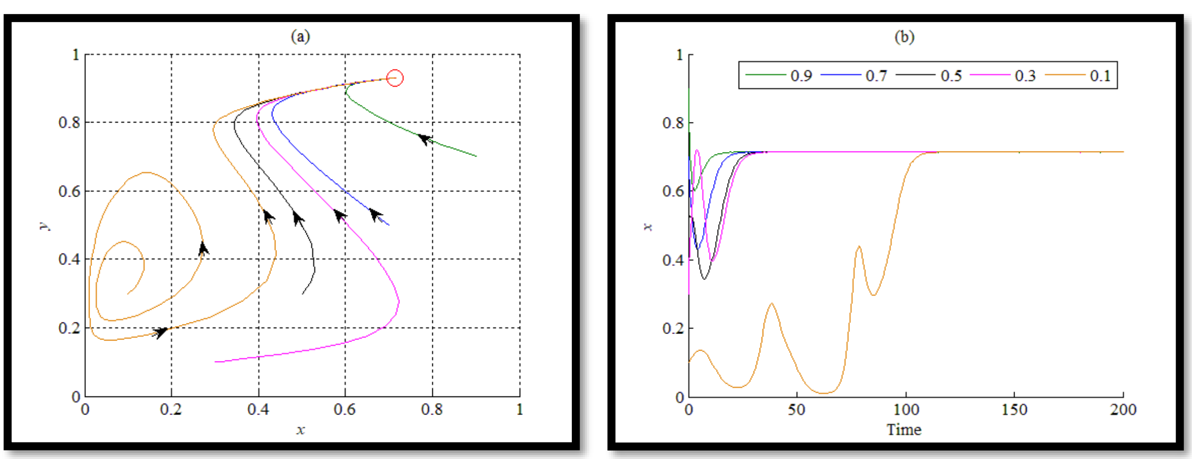

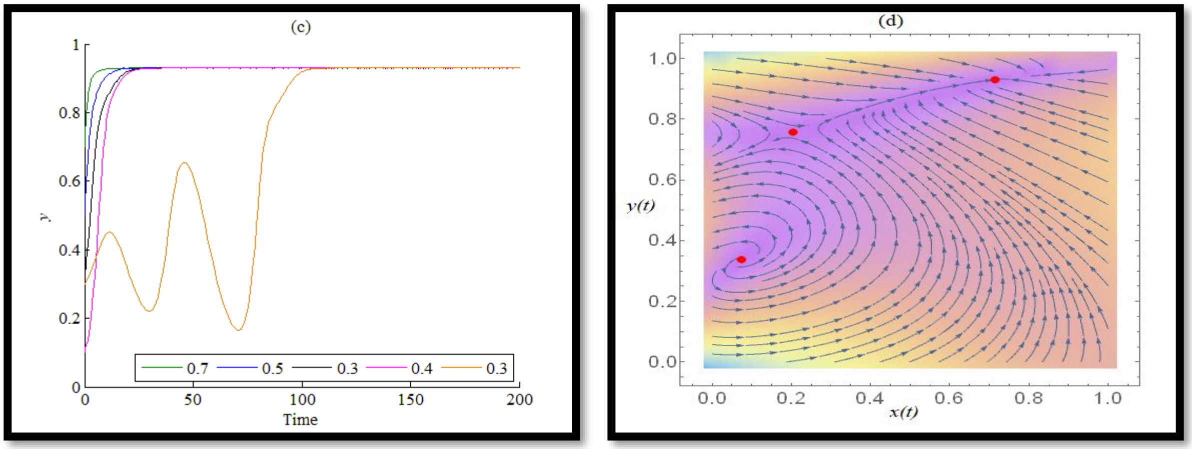

Figure 1. The trajectories of system (2) using the parameters set (24) with different initial points. (a) Approach asymptotically to a stable PSSP given by $(0.71, 0.93)$. (b) Trajectories of x versus time. (c) Trajectories of y versus time. (d) The system's direction field for the case given in (a).

System (2) has three steady-state points, as shown in Figure (1d). As illustrated in Figure (1) (a-c), the first is unstable, the second is a saddle point, and the third is the asymptotically stable point, which is proven in the direction field. Furthermore, the entire domain, with the exception of the unstable steady-states, serves as the stable PSSP's basin of attraction.

As the parameter w_0 is changed, it is discovered that the system approaches the PSSP asymptotically in the range $w_0 \in [0, 0.18]$. However, system (2) exhibits a bi-stability between two types of attractors (limit cycle and PSSP) in the range $w_0 \in [0.19, 0.37]$ depending on the initial positions. Finally, for the range $w_0 \geq 0.38$, system (2) approaches a stable limit cycle asymptotically; see Figures (2) and (3) for typical w_0 values.

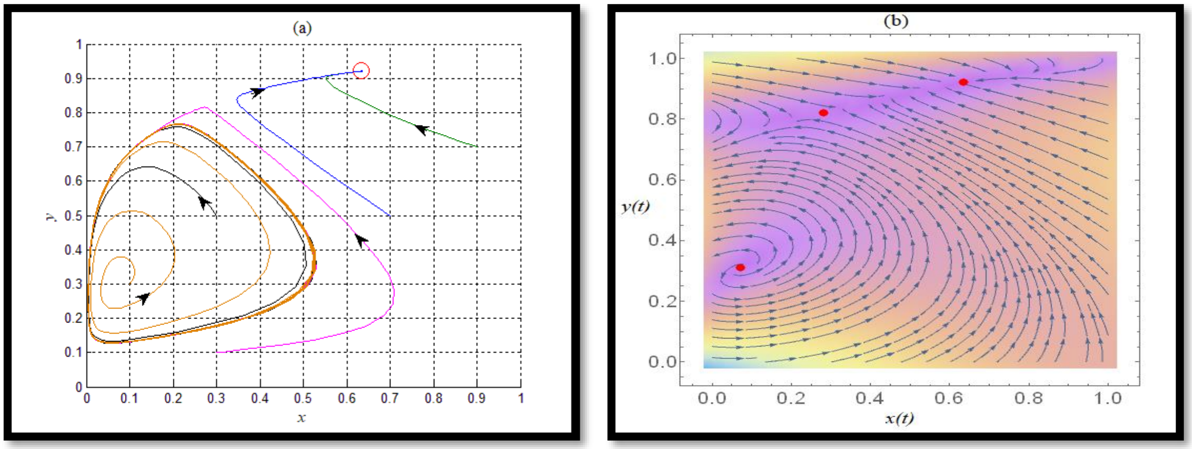

Figure 2. The trajectories of system (2) with different initial positions using the parameters set (24) with $w_0 = 0.25$. (a) The system is bi-stable between two forms of attractor limit cycle and PSSP, which are defined by (0.63, 0.92). (b) The system's direction field for the case given in (a).

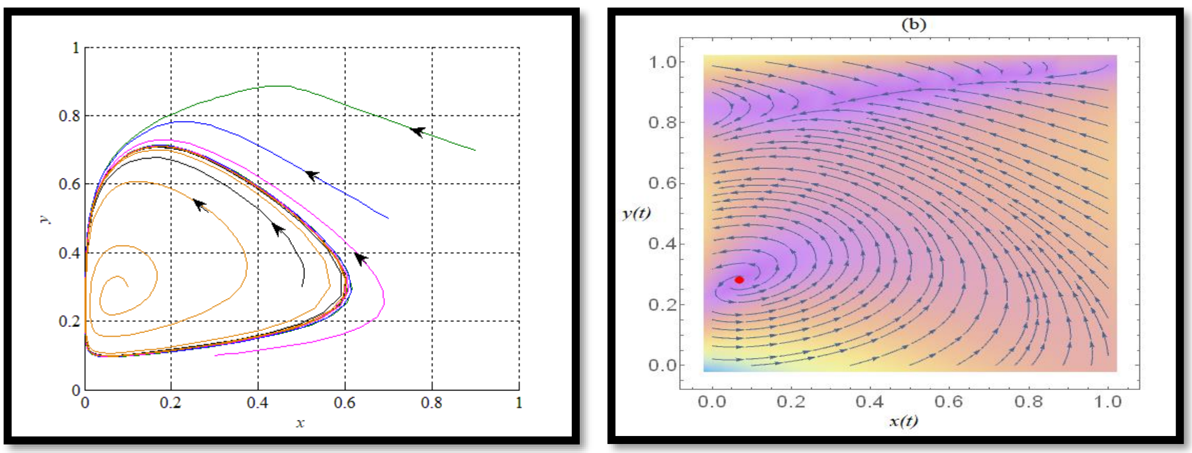

Figure 3. The trajectories of system (2) with different initial positions using the parameters set (24) with $w_0 = 0.5$. (**a**) The system is approaching a limit cycle. (**b**) The system's direction field for the case given in (a).

The basin of attraction of the limit cycle expands as the parameter w_0 increases, as shown in the phase portraits and accompanying direction fields in Figures (2) and (3). In fact, two of these PSSPs are approaching each other and then disappear letting a unique and unstable PSSP surrounded by a stable limit cycle.

The effect of changing the parameter w_1 is numerically studied, and the results obtained at typical values are shown in Figure (4a)-(4d). Figures (5a)-(5d) also show the matching direction field.

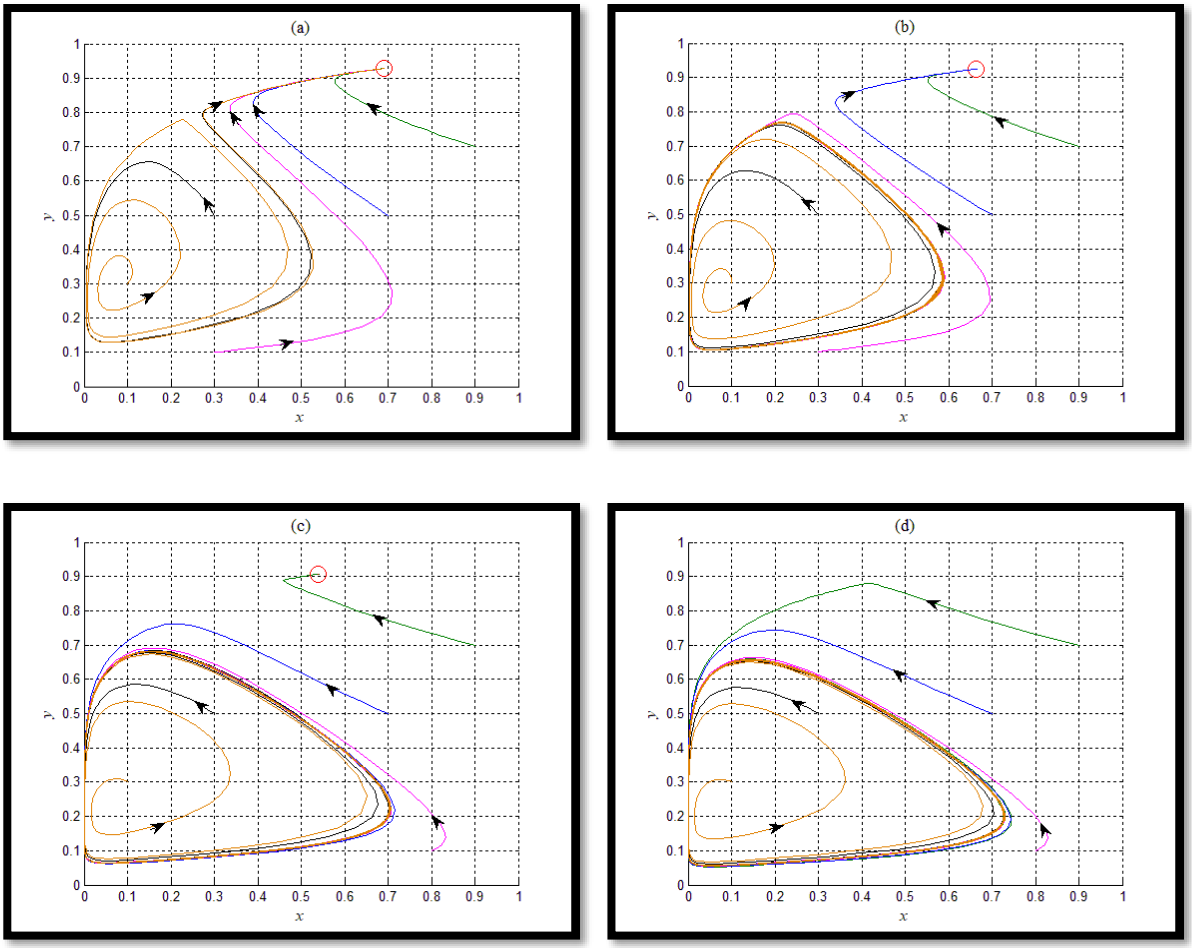

Figure 4. The trajectories of system (2) with different initial positions using the parameters set (24) with different values of w_1. (**a**) The system is approaching a PSSP that is given by $(0.69, 0.92)$, where $w_1 = 1.05$. (**b**) The system is bi-stable between a limit cycle and PSSP that is given by $(0.66, 0.92)$, where $w_1 = 1.1$. (**c**) The system is bi-stable between a limit cycle and PSSP that is given by $(0.54, 0.9)$ where $w_1 = 1.25$. (**d**) The system is approaching a limit cycle where $w_1 = 1.3$.

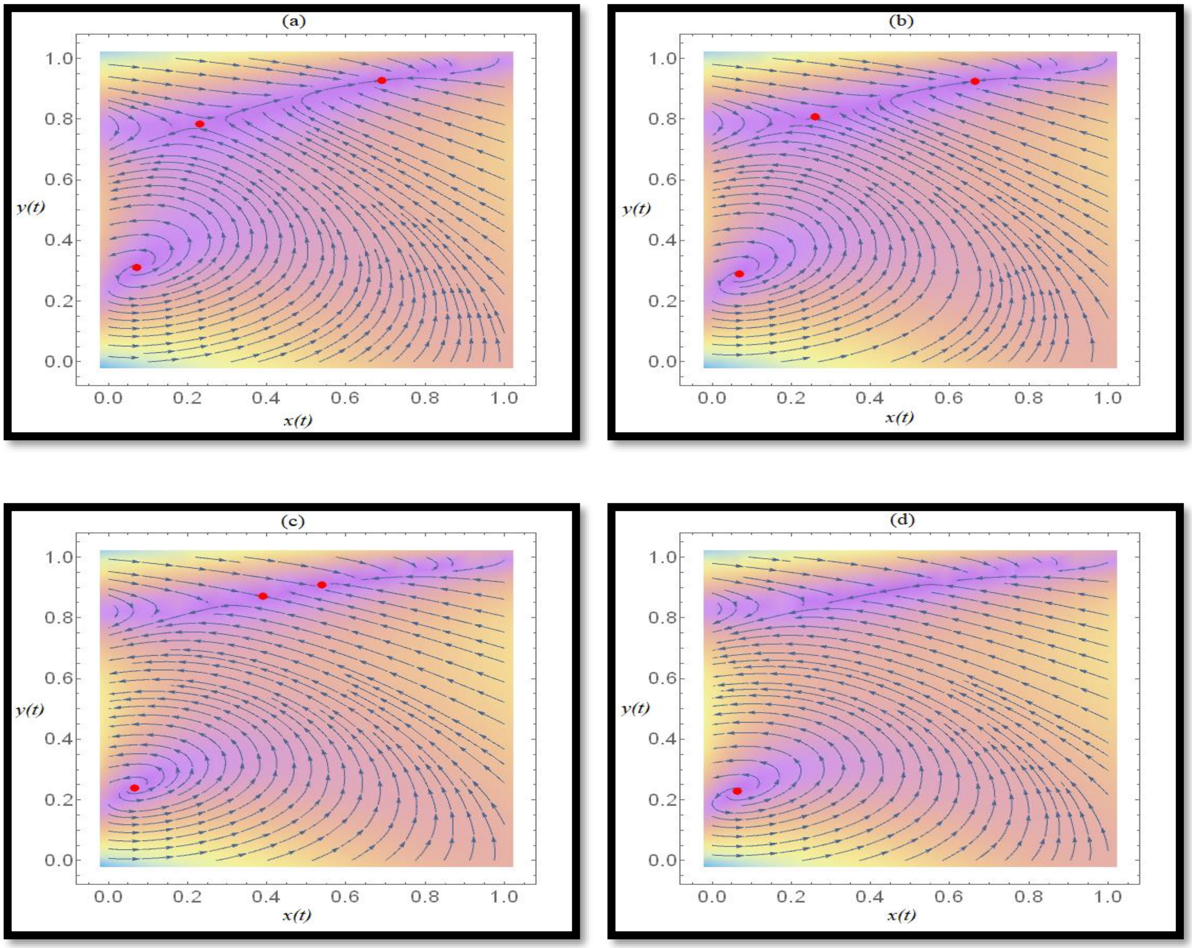

Figure 5. The system's direction field for the parameters set (24) with different values of w_1. (**a**) For $w_1 = 1.05$. (**b**) For $w_1 = 1.1$. (**c**) For $w_1 = 1.25$. (**d**) For $w_1 = 1.3$.

Increases in the value of w_1 result in the transfer of the attractor type from PSSP to the limit cycle passing through a bi-stable range, as shown in Figures (4) and (5). The effect of changing the parameter w_2 is also numerically investigated, and the resultant findings at typical values are presented in Figures (6a)-(6e), as well as the related direction field in Figures (7a)-(7e).

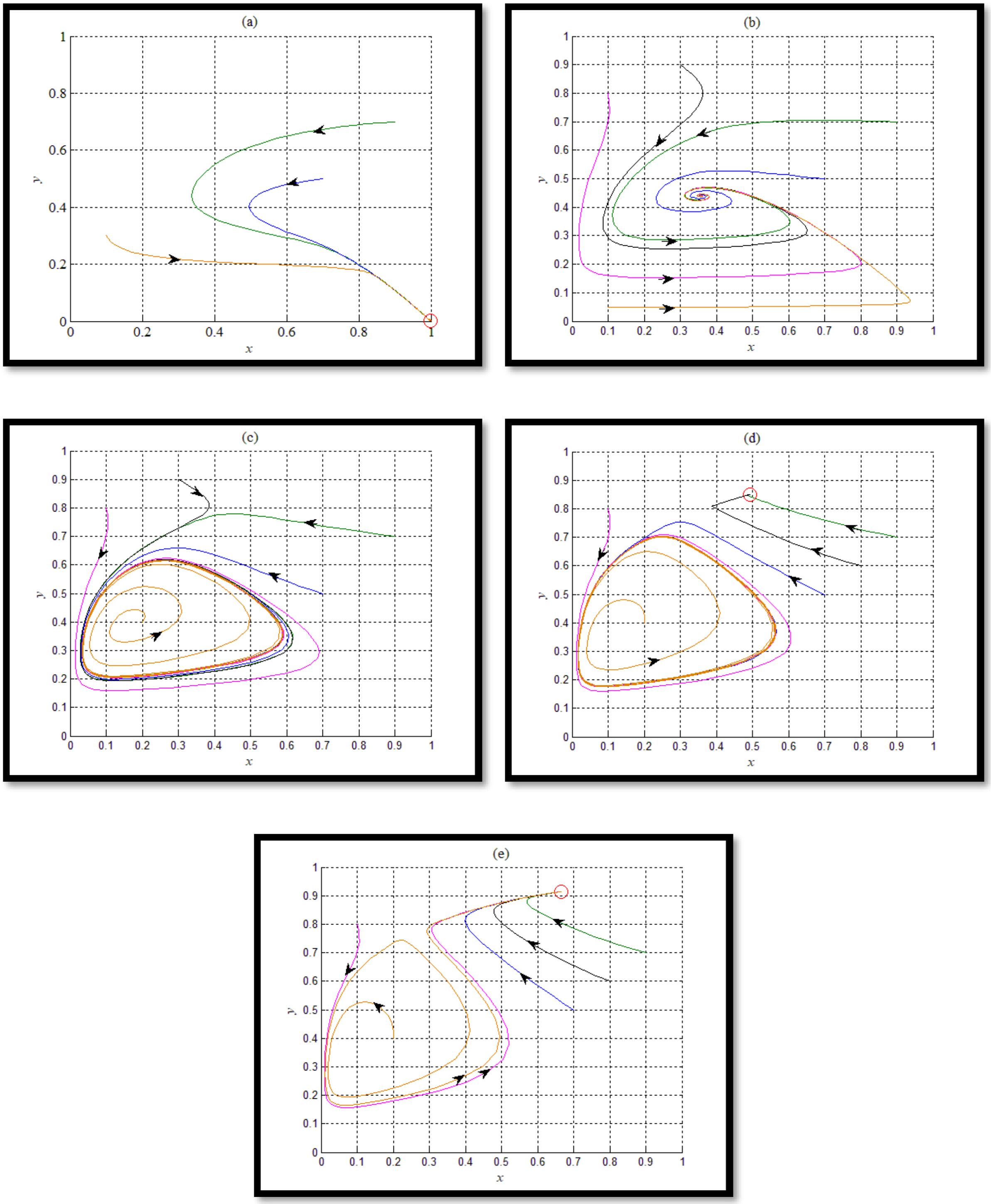

Figure 6. The trajectories of system (2) with different initial positions using the parameters set (24) with different values of w_2. (**a**) The system is approaching a ASSP where $w_2 = 0.1$. (**b**) The system is approaching a PSSP that is given by $(0.35, 0.43)$ where $w_2 = 0.2$. (**c**) The system is approaching a limit cycle where $w_2 = 0.3$. (**d**) The system is bi-stable between a limit cycle and PSSP that is given by $(0.49, 0.84)$ where $w_2 = 0.37$. (**e**) The system is

approaching a PSSP that is given by $(0.66, 0.91)$ where $w_2 = 0.45$.

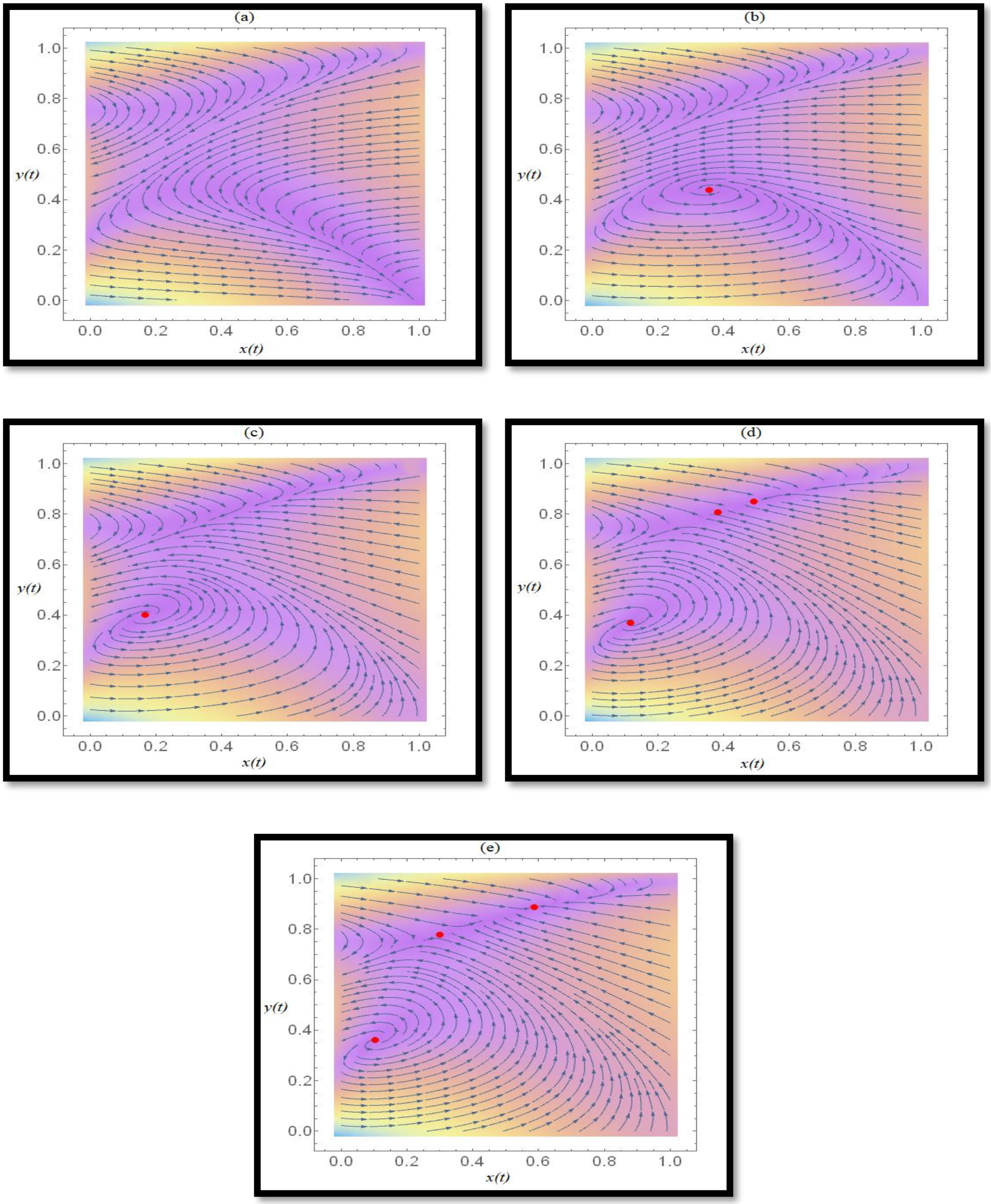

Figure 7. The system's direction field for the parameters set (24) with different values of w_2. (**a**) For $w_2 = 0.1$. (**b**) For $w_2 = 0.2$. (**c**) For $w_2 = 0.3$. (**d**) For $w_2 = 0.37$. (**e**) For $w_2 = 0.4$.

According to Figures (6) and (7), the system (2) has four bifurcation points with regard to w_2, allowing trajectories to transition from ASSP to PSSP, then to limit cycle, then to the bi-stability, and finally back to the PSSP. In reality, the system approaches the ASSP asymptotically in the range $w_2 \in (0, 0.11]$, while it approaches the PSSP in the range of $w_2 \in [0.12, 0.22]$. The system (2) then approaches the limit cycle for the range $w_2 \in [0.23, 0.36]$ asymptotically, but it has bi-stability behavior in the range $w_2 \in [0.37, 0.42]$. Finally, it approaches the PSSP for $w_2 \geq 0.43$ once more.On the other hand, an examination into the variation of the parameter w_3 was conducted, and the resulting trajectories are displayed in Figures (8) and (9) with their direction fields for the typical values.

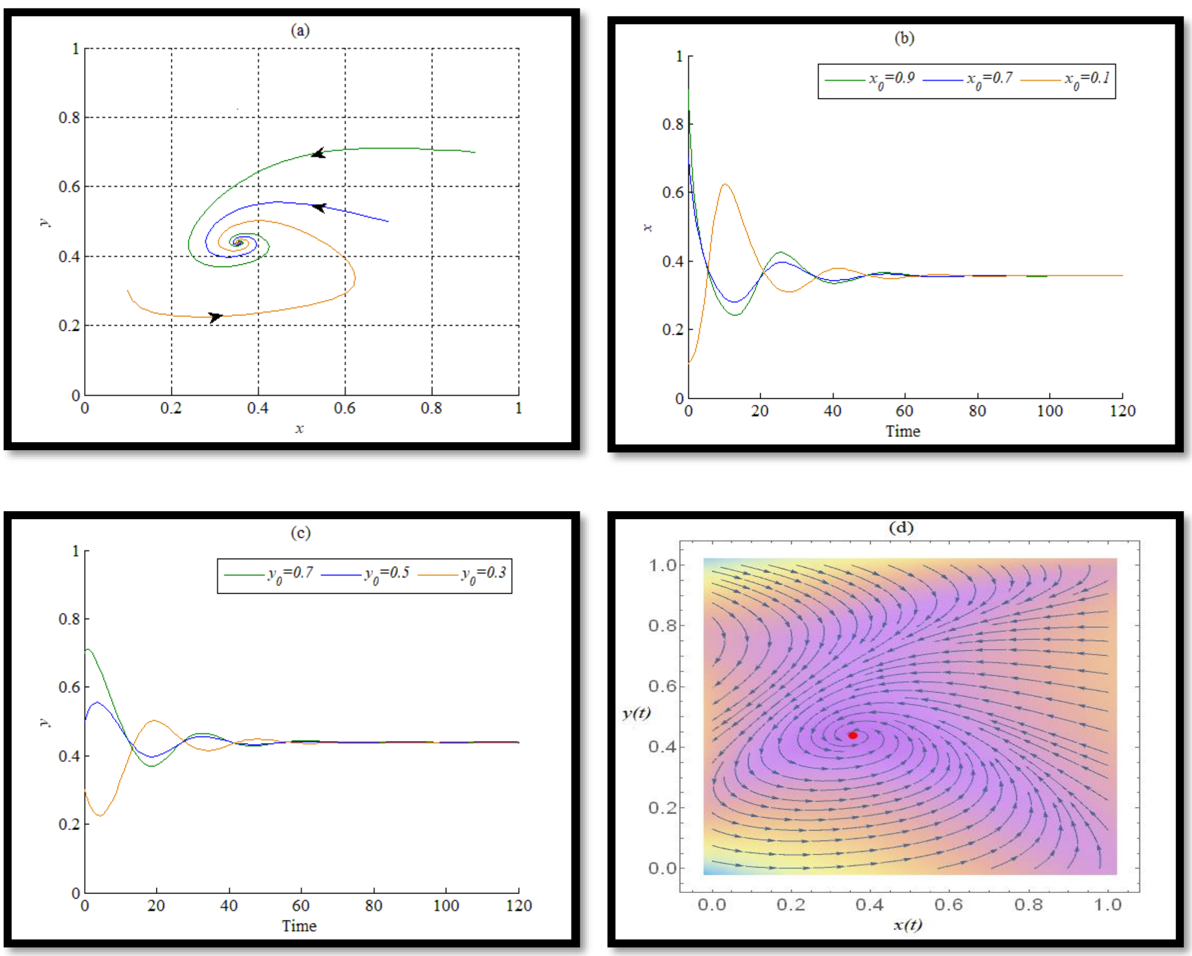

Figure 8. The trajectories of system (2) with different initial positions using the parameters set (24) with $w_3 = 0.25$. (**a**) The system is approaching a PSSP that is given by $(0.35, 0.43)$. (**b**) Trajectories of x versus time. (**c**) Trajectories of y versus time. (**d**) The system's direction field for the case given in (a).

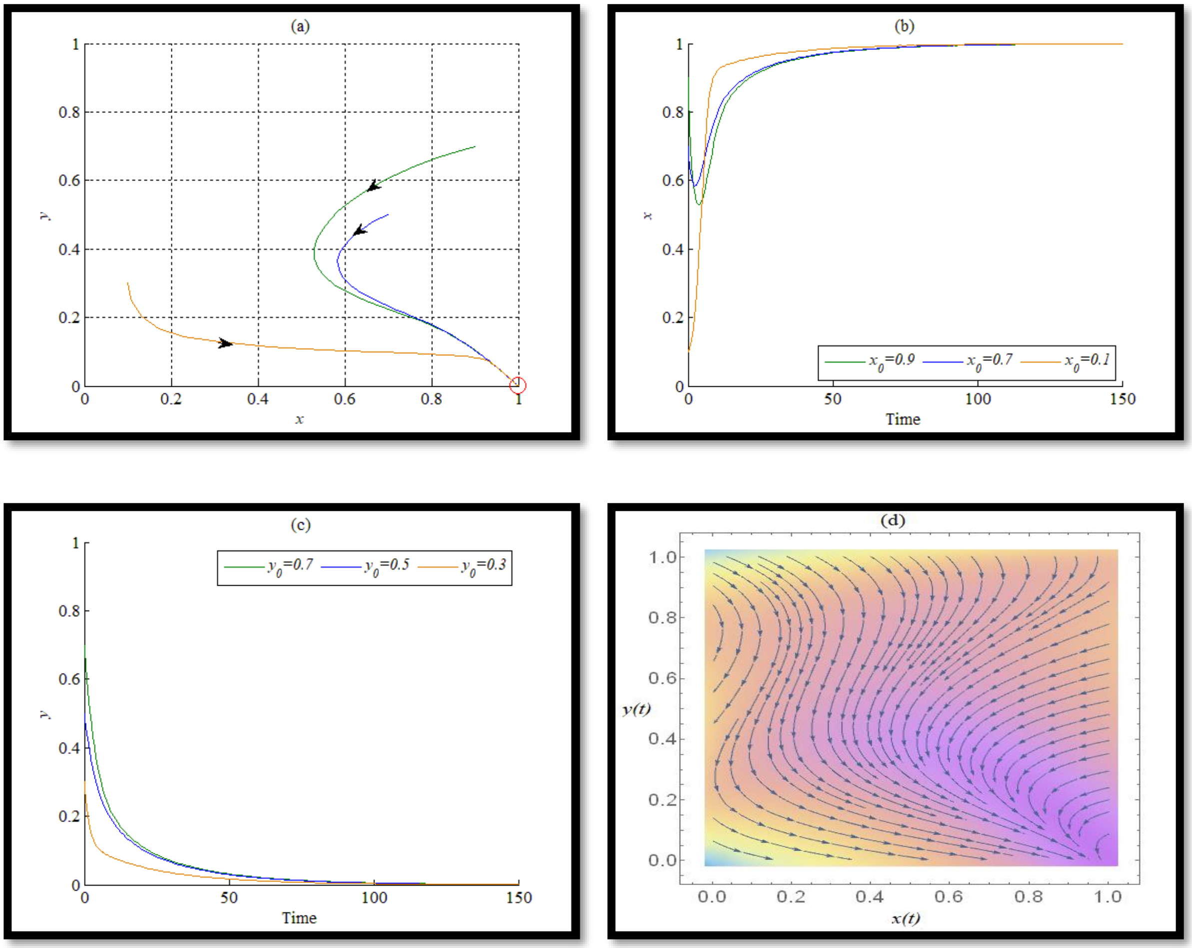

Figure 9. The trajectories of system (2) with different initial positions using the parameters set (24) with $w_3 = 0.45$. (**a**) The system is approaching a ASSP. (**b**) Trajectories of x versus time. (**c**) Trajectories of y versus time. (d) The system's direction field for the case given in (a).

Clearly, the system (2) has just one bifurcation point with regard to the parameter w_3, as shown in Figures (8) and (9) with associated direction fields, at which the solution of system (2) moves from PSSP to ASSP. In reality, it has been discovered that for the range $w_3 \in (0, 0.41]$ the system approaches asymptotically to a stable PSSP, while it approaches asymptotically to ASSP in the range $w_3 \in [0.42, 1)$. Finally, the trajectories of system (2) were explored in the situation of variable w_4, and the trajectories at typical values of w_4 with their direction fields are shown in Figure (10).

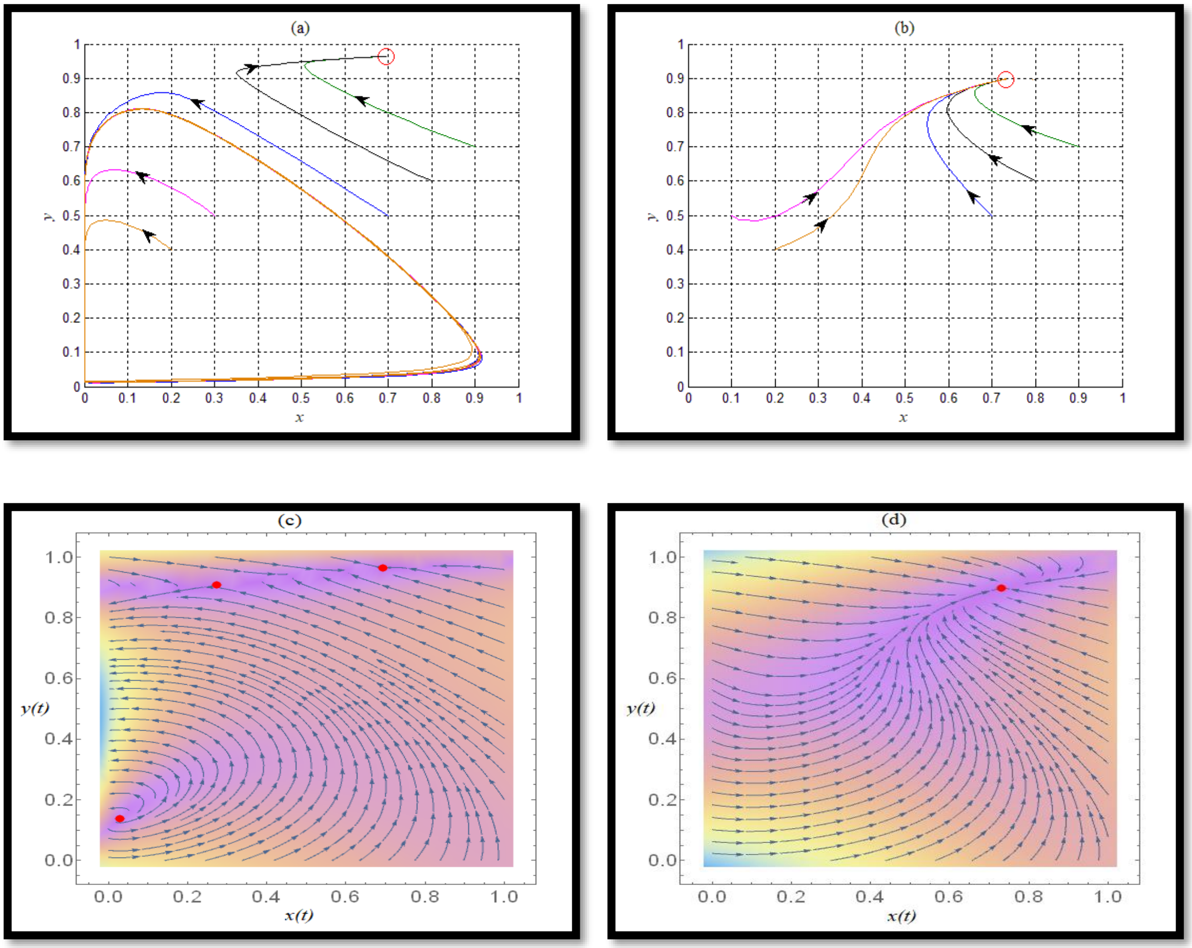

Figure 10. The trajectories of system (2) with different initial positions using the parameters set (24) with different values of w_4. (**a**) The system is bi-stable between a limit cycle and PSSP that is given by $(0.69, 0.96)$ where $w_4 = 0.1$. (**b**) The system is approaching a PSSP that is given by $(0.73, 0.89)$ where $w_4 = 0.3$. (**c**) The system's direction field for the case given in (a). (**d**) The system's direction field for the case given in (b).

System (2) contains one bifurcation point with regard to the parameter w_4, where the trajectories switch from bi-stability behavior to a stable PSSP, as shown in Figure 10. For values of w_4 in the range $w_4 \in (0, 0.14]$, the system has a bi-stability between limit cycle and stable PSSP, however, for the values in the range $w_4 \in [0.15, 1)$, it approaches a stable PSSP asymptotically.

6. DISCUSSION AND CONCLUSION

A prey-predator model including predation fear and predator-dependent refuge was proposed and studied in this work. The existence, uniqueness, and boundedness of the suggested system's solution are all examined. All feasible steady-state sites are explored for stability. The system's persistence condition has been established. The Sotomayor theorem is used to study local bifurcation. Near the ASSP, the system (2) experiences a transcritical bifurcation, while near the PSSP, it undergoes a saddle-node bifurcation. Finally, using Matlab version R2013a and Mathematica 12, the numerical simulation was performed to display the observed results based on a hypothetical set of parameters. The simulation results were investigated using phase portraits, time series, and the related direction field. It has been discovered that increasing the predation fear rate destabilizes the system, causing the dynamics to shift from approaching a stable PSSP to a stable limit cycle passing through bi-stability behavior. A similar result is produced in terms of the maximal attack rate, as illustrated in a fear rate. However, the system (2) is extremely sensitive to changes in the predator's conversion rate, so the system loses persistence at low conversion rates and endures as the conversion rate rises, confirming the persistence theoretical requirement. The system loses stability at the PSSP first and then converges to periodic as the conversion rate increases. The system then returns to PSSP stability as the conversion rate rises higher. Increased predator death rates, on the other hand, leads to extinction of predator species, and the system approaches ASSP asymptotically. Finally, increasing the half-saturation constant has a stabilizing influence on the system's behavior and the approach to PSSP solutions.

CONFLICT OF INTERESTS

The author(s) declare that there is no conflict of interests.

REFERENCES

[1] C.S. Holling, The components of predation as revealed by a study of small-mammal predation of the European pine sawfly, Can Entomol. 91 (1959), 293–320. https://doi.org/10.4039/Ent91293-5.

[2] J.D. Murray, Mathematical biology, Springer-Verlag, Berlin (1993).

[3] Y. Kuang, E. Beretta, Global qualitative analysis of a ratio-dependent predator-prey system, J. Math. Biol. 36 (1998), 389–406. https://doi.org/10.1007/s002850050105.

[4] S.-B. Hsu, T.-W. Hwang, Y. Kuang, Global dynamics of a predator-prey model with Hassell-Varley type functional response, Discrete Contin. Dyn. Syst., Ser. B 10 (2008), 857–871. https://doi.org/10.3934/dcdsb.2008.10.857.

[5] S.L. Lima, Predators and the breeding bird: behavioral and reproductive flexibility under the risk of predation, Biol. Rev. 84 (2009), 485–513. https://doi.org/10.1111/j.1469-185X.2009.00085.x.

[6] W. Cresswell, Predation in bird populations, J. Ornithol. 152 (2011), 251–263. https://doi.org/10.1007/s10336-010-0638-1.

[7] L.Y. Zanette, A.F. White, M.C. Allen, M. Clinchy, Perceived predation risk reduces the number of offspring songbirds produce per year, science. 334 (2011), 1398–1401. https://doi.org/10.1126/science.1210908.

[8] X. Wang, L. Zanette, X. Zou, Modelling the fear effect in predator–prey interactions, J. Math. Biol. 73 (2016), 1179–1204. https://doi.org/10.1007/s00285-016-0989-1.

[9] X. Wang, X. Zou, Modeling the fear effect in predator–prey interactions with adaptive avoidance of predators, Bull. Math. Biol. 79 (2017), 1325–1359. https://doi.org/10.1007/s11538-017-0287-0.

[10] S.K. Sasmal, Population dynamics with multiple Allee effects induced by fear factors – A mathematical study on prey-predator interactions, Applied Mathematical Modelling. 64 (2018) 1–14. https://doi.org/10.1016/j.apm.2018.07.021.

[11] Y. Huang, F. Chen, L. Zhong, Stability analysis of a prey–predator model with holling type III response function incorporating a prey refuge, Appl. Math. Comput. 182 (2006) 672–683. https://doi.org/10.1016/j.amc.2006.04.030.

[12] Z. Ma, W. Li, Y. Zhao, W. Wang, H. Zhang, Z. Li, Effects of prey refuges on a predator–prey model with a class of functional responses: The role of refuges, Math. Biosci. 218 (2009) 73–79. https://doi.org/10.1016/j.mbs.2008.12.008.

[13] D. Mukherjee, The effect of prey refuges on a three species food chain model, Differ. Equ. Dyn. Syst. 22 (2014), 413–426. https://doi.org/10.1007/s12591-013-0196-0.

[14] P. Panday, N. Pal, S. Samanta, J. Chattopadhyay, A three species food chain model with fear induced trophic cascade, Int. J. Appl. Comput. Math. 5 (2019), 100. https://doi.org/10.1007/s40819-019-0688-x.

[15] S. Pal, N. Pal, S. Samanta, J. Chattopadhyay, Fear effect in prey and hunting cooperation among predators in a Leslie-Gower model, Math. Biosci. Eng. 16 (2019), 5146–5179. https://doi.org/10.3934/mbe.2019258.

[16] A. Kumar, B. Dubey, Modeling the effect of fear in a prey–predator system with prey refuge and gestation delay, Int. J. Bifurcation Chaos. 29 (2019), 1950195. https://doi.org/10.1142/S0218127419501955.

[17] H. Zhang, Y. Cai, S. Fu, W. Wang, Impact of the fear effect in a prey-predator model incorporating a prey refuge, Appl. Math. Comput. 356 (2019), 328–337. https://doi.org/10.1016/j.amc.2019.03.034.

[18] S. Samaddar, M. Dhar, P. Bhattacharya, Effect of fear on prey–predator dynamics: Exploring the role of prey refuge and additional food, Chaos. 30 (2020), 063129. https://doi.org/10.1063/5.0006968.

[19] N.H. Fakhry, R.K. Naji, The dynamics of a square root prey-predator model with fear, Iraqi J. Sci. 61 (2020), 139-146 https://doi.org/10.24996/ijs.2020.61.1.15.

[20] H.A. Ibrahim, R.K. Naji, Chaos in Beddington–DeAngelis food chain model with fear, J. Phys.: Conf. Ser. 1591 (2020), 012082. https://doi.org/10.1088/1742-6596/1591/1/012082.

[21] H. Molla, Md. Sabiar Rahman, S. Sarwardi, Dynamics of a predator–prey model with Holling type II functional response incorporating a prey refuge depending on both the species, Int. J. Nonlinear Sci. Numer. Simul. 20 (2019), 89–104. https://doi.org/10.1515/ijnsns-2017-0224.

[22] L. Perko, Differential equations and dynamical systems. 3rd Edition, Springer-Verlag (2001).